Journal of Engineering Mathematics **48:** 69–91, 2004.

Salt-water up-coning during extraction of fresh water from a tropical island

LAWRENCE K. FORBES[1], GRAEME C. HOCKING[2] and SIMON WOTHERSPOON[1]
[1]*School of Mathematics and Physics, University of Tasmania, G.P.O. Box 252–37, Hobart 7001, Tasmania, Australia*
[2]*Department of Mathematics and Statistics, Murdoch University, Murdoch 6150, Western Australia*

Received 1 October 2001; accepted in revised form 29 August 2003

Abstract. Rainwater can collect in a lens-shaped region within the rock of a tropical island, and may be separated from the underlying salt water by a sharp interface. This paper presents a nonlinear theory for determining the shape of this interface. The island is assumed to be saturated with rain, and provision is made for the outflow of rain-water through the sides of the island. The effect of a bore well on the shape of the interface is investigated, and the problem is solved using a spectral method. An integral-equation method is also presented for the case when the island has infinite width.

Key words: groundwater flow, integral equation, interface, spectral methods, up-coning, withdrawal flows

1. Introduction

The extraction of fluid from reservoirs, ponds or horizontal aquifers is an important problem in fluid mechanics, and is of considerable practical interest. Much theoretical work has been undertaken on problems of this type, over the past decade or so, and significant gains in understanding have been made.

Withdrawal of a fluid from a reservoir is perhaps the simplest situation to describe, although the apparent simplicity of the problem description belies the difficulty experienced in solving the problem and interpreting the results. Imagine a very large body of water, such as a reservoir, in which all the fluid is at rest. There is a free surface bounding the fluid from above, but since the fluid is at rest, this surface is simply horizontal. Now suppose that fluid is withdrawn from the reservoir, through some sort of extraction outlet situated within the fluid. The free surface deforms in response to this disturbance, and a velocity flow field is set up in the fluid. A key task is to find the new shape assumed by the disturbed free surface. Reservoir problems are usually modelled assuming potential flow of an inviscid fluid with a Bernoulli boundary condition and a kinematic condition at the free surface.

If the reservoir is stratified so that it contains water in two horizontal layers, then an interface will be present between the upper (lighter) fluid and the lower (heavier) one. If now fluid is selectively withdrawn from one of the layers, the interface deforms in response to this disturbance. It is important to find the new shape of this interface, and in particular to determine whether situations can arise in which the interface itself is drawn into the extraction outlet. In that case, the withdrawal process would not just involve fluid from the one layer in which the outlet was located; instead, some sort of break-through event would occur, so that fluid from both layers would be extracted.

It follows that a practical design criterion in reservoir engineering is to find the maximum pumping rate permissible, before break-through occurs and both fluids begin to be extracted. This is the situation in reservoirs where a highly saline layer of fluid has formed beneath the upper fresh layer. In that case, extraction of the fresh water for town use cannot involve the lower salty fluid. A similar consideration occurs in the management of cooling ponds.

Although reservoir withdrawal problems are simple to formulate mathematically, it is nevertheless known that at least three different types of solution behaviour are possible, depending upon the extraction pumping rate. If the extraction occurred through a long horizontal perforated pipe, the fluid velocity field would be largely independent of the coordinate in the direction along the pipe. In that case, the flow could be regarded as two-dimensional.

For these two-dimensional flows, Tuck and Vanden-Broeck [1] showed that the system of governing equations permits two different solutions, the first of which occurs at low pumping rate, and involves a weakly disturbed interface with a stagnation point located immediately above the extraction pipe (which is present in the lower fluid layer). This solution type was studied in more detail by Hocking and Forbes [2], who demonstrated numerically that there is a maximum pumping rate, beyond which steady-state solutions of this type are apparently not possible. Those authors were not able to identify a physical cause for this limitation. In subsequent work, Forbes and Hocking [3] suggested that the maximum pumping rate might be a consequence of a mathematical fold singularity in the solution, associated with the presence of multiple steady solutions.

The second solution type identified by Tuck and Vanden-Broeck [1] is a steady situation in which the interface is drawn vertically downwards into a cusp. This second flow type occurs at one isolated value of the pumping rate only, and is mathematically unrelated to the first solution type that has a stagnation point on the interface. The pumping rate at which this solution occurs is significantly higher than the maximum rate for the first solution type, and so there is a window of pumping rates in which steady flows appear not to be possible.

The isolated cusped solution of Tuck and Vanden-Broeck [1] was explained by Hocking [4]. He showed that the formation of a downward vertical cusp at the fluid interface, at the unique value of the pumping rate, represents the incipient break-through event; for larger pumping rates, both the lower and the upper fluid would be drawn directly into the extraction sink, along with the interface itself. This is then the third steady solution type possible for this reservoir problem.

There has also been a significant amount of work in the past decade to extend the results of Tuck and Vanden-Broeck [1] and Hocking [4] to the case of three-dimensional withdrawal flow into an isolated extraction outlet. Forbes and Hocking [5] considered an axisymmetric flow problem involving fluid withdrawal through a point sink, using this mathematical singularity to represent an actual outlet. They found solutions with a stagnation point at the free surface, similar to the corresponding two-dimensional situation discussed by Tuck and Vanden-Broeck [1] and Hocking and Forbes [2]. There is again a maximum pumping rate beyond which steady solutions do not exist, although in this three-dimensional problem there is a clear physical cause for this maximum, associated with the formation of a secondary stagnation line at the surface and the onset of wave breaking. Unlike the two-dimensional flow case, however, the three-dimensional solutions so far show no evidence of cusped surface shapes similar to those discovered by Tuck and Vanden-Broeck [1]. Additionally, solutions analogous to those of Hocking [4], that involve both the upper and lower fluids being drawn down into the extraction sink, have not been found for three-dimensional axisymmetric flow.

Recent work of Forbes and Hocking [6] suggests that such steady solutions may perhaps not even exist.

By contrast, when the extraction point sink is located *above* the interface between the two fluids, it is known that a cusp may be produced at the interface in axisymmetric three-dimensional flow, as the heavier lower fluid is drawn *upwards* toward the sink. For axisymmetric withdrawal involving slow viscous (Stokes) flow of a two-fluid system, Lister [7] computed interface profiles up to and including super-critical extraction rates, for which both fluids were withdrawn. This model was chosen for its relevance to the geological situation of an erupting volcano. Similarly, the axisymmetric deformation of a gas-liquid interface by a point sink located above the interface, in the gas layer, has been studied by Singler and Geer [8].

The present paper is concerned with extraction of a fluid from a porous medium. This situation is related mathematically to the reservoir models discussed above, since it also involves potential flow. In the present case, however, the condition at the interface is different. A classical text that discusses groundwater applications is the book by Muskat [9] and subsequent works on flow in porous media include books by Bear [10] and Dagan [11], for example. In situations where a horizontal layer of oil is present in a porous rock, and is supported below by a large volume of water also trapped in the rock, a horizontal interface may exist between the water and the oil. When an extraction point is introduced into the oil and pumping begins, the interface is drawn upward towards the withdrawal region, forming a 'water cone'. If pumping is too severe, break-through can again occur and water from the underlying layer is extracted along with the oil.

Axisymmetric withdrawal solutions for the water coning problem were computed by Lucas, Blake and Kucera [12], using an integral equation approach. They obtained steady-state solutions, valid up to pumping strengths at which the interface forms an upward vertical cusp. For pumping rates greater than this limiting value, the flow might become unsteady, or perhaps involve the simultaneous withdrawal of both fluids (similar to the situation described by Lister [7] and Hocking [4]). Lucas and Kucera [13] later extended this work to allow for more general geometries in an oil extraction field. A similar, two-dimensional, water coning situation was studied by Zhang *et al.* [14], who also found that steady solutions are ultimately limited at a pumping rate at which the water-oil interface forms an upward vertical cusp. Their solution technique did not rely on numerical schemes, but instead involved a fully analytical approach based on a hodograph transformation. Their results give confidence in the predictions of numerical solution methods for these problems.

A numerical scheme similar to that of Lucas and Kucera [13] was used by Forbes [15], to design flow fields for the efficient extraction of low-grade underground ore by mineral leaching. In this application, the flow type is analogous to the third type of solution for withdrawal from reservoirs found by Hocking [4], in which both upper and lower fluids are extracted simultaneously in a supercritical flow.

It is often desired to extract fresh groundwater from porous rock for domestic use. The fresh water may occur in a horizontal layer within the rock, above a lower layer of salty water. Approximate solutions for the interface between fresh and salty water in coastal aquifers in the two-dimensional case are given by Bear [10, pp. 559–563] and Dagan [11, pp. 216–239], and show that the interface in this zone is a portion of an inverse parabola. A similar feature is seen for the more complicated axisymmetric flow discussed in the present paper, near the coastal region. When the upper fresh water is withdrawn, the interface between the fresh and salty fluid layers is also drawn upwards, and forms a vertical cone precisely as in the case of oil recovery.

Ma *et al.* [16] present a model of salt-water up-coning caused by extraction from an aquifer. The book by Holzbecher [17, Chapter 12] gives an approximate numerical solution for two-dimensional unsteady up-coning withdrawal. In that calculation, a steady-state was sought as the long time limit of the numerical results, but was clearly difficult to obtain. One purpose of the present paper is to seek such steady solutions directly, for a three-dimensional flow. The formation of a vertical cone in withdrawal from a two-phase aquifer has likewise been considered by Huyakorn *et al.* [18], using a finite-element method to solve the unsteady field equations. Their method shows a limiting profile with a vertical cusp, for axi-symmetric geometry. For larger pumping rates, they apparently computed unsteady extraction of both the water in the upper layer and the salty lower fluid. Bower *et al.* [19] have given an approximate analytical method for determining the critical pumping rate in a confined aquifer, using an assumed form for the interface shape.

Fresh water resources must be managed carefully by communities living on small ocean-bound islands, as has been discussed by Langevin *et al.* [20]. The fresh water is usually located in a lens that floats on the underlying sea-water within the island. The presence of artificially constructed canals in the island and the process of extraction of the water for drinking purposes may both disturb the shape of the fresh-water lens.

It is of practical importance to know the precise location of the fresh-water salt-water interface within the island. An example of an experimental survey technique for determining this information is given by Ruppel *et al.* [21]. There is a simple classical formula for determining the interface height, known as the Ghyben-Herzberg equation, and it may be derived from texts such as [22, p. 402] and [23, p. 175] for example. The formula assumes a sharp interface between the two different fluids, and gives an approximation to the interface height away from coastal regions, based on a simple hydrostatic pressure balance. A comprehensive review of the Ghyben-Herzberg approach is given by Essaid [24], and a finite-difference model is developed and applied to actual aquifers in the Hawaiian Islands. Fresh-water extraction from the Ghyben-Herzberg fresh water lens is considered using a simplified one-dimensional theory by Nutbrown [25], and a more elaborate two-dimensional anisotropic model is given by Padilla and Cruz-Sanjulián [26], who solved their system of equations with a finite-element method.

In the present paper, an idealized model of a tropical island is considered, in which the island is modelled as a circular cylinder with a flat top. There is a lens of fresh water within the island, floating above the sea water, and a sharp interface separates the two regions. Extraction occurs at the island centre-line, at some specified height above sea level, and the extraction well is represented by an equivalent mathematical point sink. Re-charge of the fresh-water aquifer occurs by rainfall, which is assumed to be so plentiful that the surface of the aquifer coincides with the top of the island; excess rainfall runs away to the ocean, in a very short time scale. The system of governing equations for this situation is outlined in Section 2.

It has been found that determining the flow within the island and the location of the interface is generally a mathematically ill-conditioned problem; see [27, p. 309]. This fact has been commented on previously by Wikramaratna and Wood [28], for problems of this type, and is therefore not unexpected. These authors observe that spurious oscillations in the numerical results are often produced, and similar difficulties have been encountered here also. In fact, a range of different island shapes and numerical methods has been tried for this problem, and the present paper makes use of two such numerical schemes. The first is a spectral Galerkin method for the idealized island geometry considered here, and is presented in Section 3. This scheme is capable of great accuracy, but is usually ill-conditioned in cases

of physical interest, giving rise to spurious oscillations near the coastal zone and the extraction region. A regularization strategy is used to control these oscillations.

A second numerical method is outlined in Section 5, and makes use of a boundary-integral approach in a region closer to the extraction zone at the island's centre. An analysis in Section 4 confirms the results that are presented in Section 6. Some concluding remarks and observations are given in Section 7.

2. The governing equations

The problem is first described in dimensional variables. The island is taken to have a circular cylindrical shape, of radius A. It is assumed to have vertical sides, for simplicity, and to rise a height H above the sea level. A Cartesian coordinate system is located with the origin at sea level and the z-axis pointing vertically up the central axis of the cylindrical island. The horizontal top surface of the island, at height $z = H$, is kept continually moist by frequent rain showers, and fluid within the rock of the island is drawn downwards, in the negative z-direction, by the constant acceleration g of gravity. An extraction well is present down the z-axis, and withdraws fluid from a point on the z-axis at height L above the sea level. At that point, there is an effective point sink of total withdrawal strength Q_s.

Let us denote the upper fresh water layer as "fluid 1", and the lower salty layer as "fluid 2". According to Darcy's law, the seepage velocity vector $\mathbf{q}_i$ in each fluid layer $i = 1, 2$ is related to the pressure p_i in each layer by the formula

$$\mathbf{q}_i = -K\nabla(p_i + \rho_i g z); \tag{2.1}$$

see [11, p. 92]. Here, the constant K (m^3 s/kg) represents the total permeability of the rock (permeability divided by fluid viscosity), and ρ_i are the densities of the fluids in each layer, $i = 1, 2$. It is assumed that the rock is fully saturated, so that the incompressibility conditions

$$\nabla \cdot \mathbf{q}_i = 0 \tag{2.2}$$

hold, in each fluid layer $i = 1, 2$.

Non-dimensional variables are now introduced, by scaling all lengths relative to the island height H, and velocity relative to the quantity $\rho_1 g K$, which is the characteristic seepage speed of water (in layer 1) due to gravity. The pressures p_i are referenced to the term $\rho_1 g H$. The solutions to this problem may now be seen to depend on the four non-dimensional parameter groups

$$\alpha = \frac{A}{H}, \qquad D = \frac{\rho_2}{\rho_1}, \qquad \lambda = \frac{L}{H}, \qquad \mu = \frac{Q_s}{\rho_1 g H^2}.$$

The quantity α is the dimensionless radius of the island, which in these new dimensionless variables now has height 1 above sea level, and D denotes the ratio of densities of salt water to fresh water, so that $D > 1$. The extraction sink is at dimensionless height λ above sea level, within the island, and its extraction rate is μ. A sketch of the geometry illustrating these non-dimensional variables is given in Figure 1.

In dimensionless variables, Darcy's law (2.1) is now written

$$\mathbf{q}_i = -\nabla\Phi_i, \qquad i = 1, 2, \tag{2.3}$$

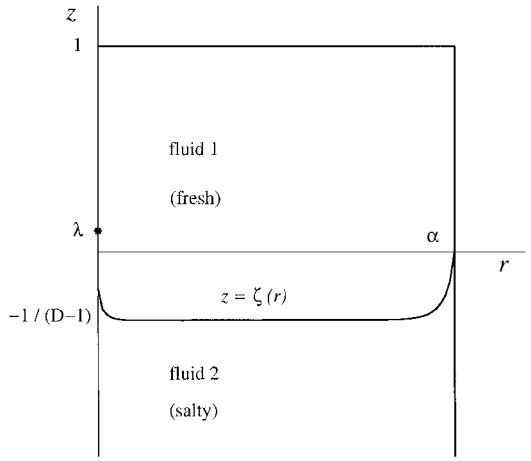

Figure 1. A schematic diagram of the non-dimensionalized flow problem, for an island of finite radius α. (The interface is taken from an actual solution with radius $\alpha = 25$, density ratio $D = 4$, sink height $\lambda = 0{\cdot}1$ and strength $\mu = 1{\cdot}2$).

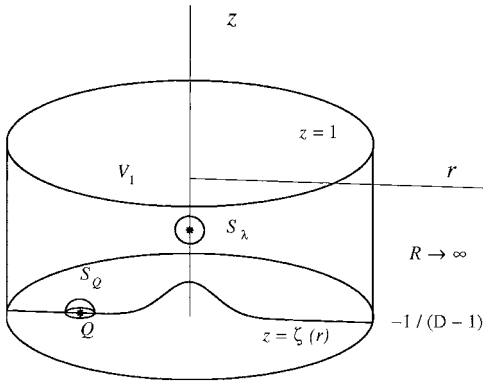

Figure 2. The volume V_1 containing the upper fresh-water layer, and its boundary surfaces ∂V_1 used in the derivation of the integral equation in Section 5.

in which the total pressure head in each fluid is defined to be

$$\Phi_1 = p_1 + z, \qquad \Phi_2 = p_2 + Dz. \tag{2.4}$$

It follows from Equations (2.3) that the pressures Φ_i act as velocity potentials in each layer, $i = 1, 2$. In the lower (salty) layer 2, it is evident that $\Phi_2 = 0$ on the sea surface $z = 0$ external to the island, and so for a steady-state solution, it must be the case that $\Phi_2 = 0$ throughout the entire lower layer. Thus there is no movement of salty water in the steady-state situation, so that $\mathbf{q}_2 = \mathbf{0}$. Equations need therefore only be developed for the fluid in the fresh water lens (layer 1).

By virtue of Darcy's law (2.3) and the incompressibility condition (2.2), it follows that the total pressure head Φ_1 satisfies Laplace's equation in cylindrical polar coordinates (r, θ, z)

$$\nabla^2 \Phi_1 = \frac{1}{r}\frac{\partial}{\partial r}\left(r\frac{\partial \Phi_1}{\partial r}\right) + \frac{\partial^2 \Phi_1}{\partial z^2} = 0 \tag{2.5}$$

in fresh water layer 1. The axisymmetric nature of the solution has been taken into account in Equation (2.5). Symmetry requires that the condition

$$\partial \Phi_1 / \partial r = 0 \qquad \text{on } r = 0 \tag{2.6}$$

be satisfied on the axis of the cylindrical island.

The top of the island is subject to sufficient rainfall to keep the entire region above the interface always saturated. Excess rainwater simply runs away to the ocean, on a time scale much shorter than typical times associated with the movement of groundwater. Thus the fluid at the top of the island must be at atmospheric pressure, and so the fluid pressure p_1 there must be zero. Thus

$$\Phi_1 = 1 \qquad \text{on } z = 1. \tag{2.7}$$

Similarly, because the sides of the island are saturated and exposed to the atmosphere, the pressure there is likewise zero, so that

$$\Phi_1 = z \qquad \text{on } r = \alpha, \qquad 0 < z < 1. \tag{2.8}$$

Near the point sink, the potential Φ_1 has the behaviour

$$\Phi_1 \to -\frac{\mu}{4\pi\sqrt{r^2 + (z-\lambda)^2}} \qquad \text{as } (r, z) \to (0, \lambda). \tag{2.9}$$

The fresh water lens (layer 1) is bounded below by an interfacial surface $z = \zeta(r)$, that separates it from the stationary salt-water layer underneath. There is no component of flow normal to this interface, and so the kinematic condition there becomes

$$\frac{\partial \Phi_1}{\partial z} = \frac{\partial \Phi_1}{\partial r}\frac{\mathrm{d}\zeta}{\mathrm{d}r} \qquad \text{on } z = \zeta(r) \tag{2.10}$$

There is also a dynamical condition to be satisfied on this interface, since fluid pressures there must balance. Therefore, $p_1 = p_2$ across the interface, and so Equations (2.4), and the fact that $\Phi_2 = 0$ everywhere in the salty layer, yield the condition

$$\Phi_1 = -(D-1)z \qquad \text{on } z = \zeta(r) \tag{2.11}$$

The solution to the problem of flow within the fresh water lens is determined by finding a potential Φ_1 and an interface shape $z = \zeta(r)$ that satisfy the system of Equations (2.5)–(2.11). To this system must be added the auxiliary condition

$$\zeta(\alpha) = 0, \tag{2.12}$$

which expresses the fact that the interface rises to the sea level at the edge of the island $r = \alpha$.

3. Spectral Galerkin method for island of finite width

In this section, a spectral method is presented for the solution of the problem in Section 2, in which the island has finite width α. A similar, simpler scheme is discussed for two-dimensional problems in the book by Holzbecher [17, p. 199], although the present method is designed for axisymmetric flow in three-dimensional geometry. Nevertheless, it will be seen that the problem is ill-conditioned, and this fact has been noted by other researchers such as Wikramaratna and Wood [28]. Ill-conditioning refers to the fact that small changes in flow parameters can cause large changes in the solution, and happens when the mathematical problem is nearly singular. Physically, this occurs here when the density ratio D is close to unity, so that very small errors will lead to large changes in the location of the interface. Accordingly, a regularization scheme is needed, to stabilize the results.

To begin, suppose that the point sink at $(r, z) = (0, \lambda)$ is removed from the mathematical problem; that is, set the sink strength $\mu = 0$ in Equation (2.9). Then it is possible to write down at once a formal solution to Laplace's equation (2.5), that satisfies the symmetry condition (2.6), the top condition (2.7) and the side condition (2.8). In dimensionless variables, this solution is

$$\Phi_1^{(1)}(r, z) = z + \sum_{n=1}^{\infty} C_n J_0\left(j_{0,n}\frac{r}{\alpha}\right)\sinh\left(j_{0,n}\frac{1-z}{\alpha}\right). \tag{3.1}$$

This result (3.1) has been obtained in the usual way by means of separation of variables. The symbol J_0 denotes the Bessel function of the first kind, of zeroth order, as may be found in [29, Chapter 9] for example, and $j_{0,n}$ refers to its n-th zero. The real constants C_n are as yet unknown.

To the solution (3.1), it is now necessary to add a function that accounts for the presence of the sink at $(r, z) = (0, \lambda)$. Thus we seek a function of the form

$$\Phi_1^{(2)}(r, z) = -\frac{\mu}{4\pi\sqrt{r^2 + (z-\lambda)^2}} + P(r, z; \lambda) \tag{3.2}$$

that satisfies Laplace's equation (2.5), the sink condition (2.9) and the symmetry requirement (2.6). It is also required to satisfy a homogeneous equivalent of the side-wall condition (2.8), namely

$$\Phi_1^{(2)} = 0 \qquad \text{on } r = \alpha.$$

The function $\Phi_1^{(2)}$ in Equation (3.2) will not obey a corresponding homogeneous condition on the top of the island, at $z = 1$, and this additional constraint must be imposed later.

The equations obeyed by the quantity $P(r, z; \lambda)$ in the expression (3.2) are solved using Fourier transforms. The calculation is straightforward, if lengthy, and the final result is

$$\Phi_1^{(2)}(r, z) = -\frac{\mu}{4\pi\sqrt{r^2 + (z-\lambda)^2}} + \frac{\mu}{2\pi^2}\int_0^\infty \frac{I_0(\omega r)}{I_0(\omega\alpha)} K_0(\omega\alpha)\cos\big(\omega(z-\lambda)\big)\,\mathrm{d}\omega. \tag{3.3}$$

The functions I_0 and K_0 in this expression (3.3) are the modified Bessel functions of the first and second kinds, respectively, of order zero; these functions may be found in [29, p. 374].

It is also necessary to add an image term to the potential, so as to satisfy the homogeneous Dirichlet condition at the top of the island (corresponding to Equation (2.7)). Physically, this corresponds to an image *source* being located at the point $(r, z) = (0, 2 - \lambda)$. The additional function is thus

$$\Phi_1^{(3)}(r, z) = \frac{\mu}{4\pi\sqrt{r^2 + (z-2+\lambda)^2}} - \frac{\mu}{2\pi^2}\int_0^\infty \frac{I_0(\omega r)}{I_0(\omega\alpha)} K_0(\omega\alpha)\cos\big(\omega(z-2+\lambda)\big)\,\mathrm{d}\omega. \tag{3.4}$$

Laplace's equation (2.5) is linear, and so its total solution may be constructed by superposition of the three functions in Equations (3.1), (3.3) and (3.4). The final result is

$$\begin{aligned}\Phi_1(r, z) \;=\; & z + \frac{\mu}{4\pi}\left[\frac{1}{\sqrt{r^2 + (z-2+\lambda)^2}} - \frac{1}{\sqrt{r^2 + (z-\lambda)^2}}\right] \\ & - \frac{\mu}{\pi^2}\int_0^\infty \frac{I_0(\omega r)}{I_0(\omega\alpha)} K_0(\omega\alpha)\sin\big(\omega(z-1)\big)\sin\big(\omega(1-\lambda)\big)\,\mathrm{d}\omega \\ & + \sum_{n=1}^{\infty} C_n J_0\left(j_{0,n}\frac{r}{\alpha}\right)\sinh\left(j_{0,n}\frac{1-z}{\alpha}\right).\end{aligned} \tag{3.5}$$

It may now be verified directly that the solution (3.5) indeed satisfies Laplace's equation (2.5) and the boundary conditions (2.6)–(2.9).

It remains to satisfy the two conditions (2.10) and (2.11) on the unknown interface location $z = \zeta(r)$, which is likewise represented in the spectral form

$$\zeta(r) = \sum_{n=1}^{\infty} B_n J_0\left(j_{0,n}\frac{r}{\alpha}\right). \tag{3.6}$$

This expression (3.6) also has the advantage that it satisfies the auxiliary condition (2.12) identically.

A Galerkin method is now used to satisfy the remaining boundary conditions (2.10) and (2.11), based on the representations (3.5) and (3.6) for the unknown potential and interface location, respectively.

A vector of unknowns $\mathbf{u}$ of length $2N$ is created from the first N coefficients in each spectral representation; thus

$$\mathbf{u} = \left[B_1, B_2, \ldots, B_N; C_1, C_2, \ldots, C_N\right]^T. \tag{3.7}$$

An initial estimate is made for the coefficients in the vector (3.7), and on this basis, the interface location $\zeta(r)$ can be computed directly from Equation (3.6). Its derivative $\zeta'(r)$ can also be computed by direct differentiation of the expression (3.6). Similarly, the surface potential $\Phi_1(r, \zeta)$ and the two velocity components $u_1 = -\partial\Phi_1/\partial r$ and $w_1 = -\partial\Phi_1/\partial z$ at the interface may be obtained directly from Equation (3.5) (and Darcy's law (2.3)).

The estimate of the coefficients in the vector (3.7) of unknowns is updated iteratively, by requiring the error vector

$$\mathbf{E} = \left[E_1, E_2, \ldots, E_N; E_{N+1}, E_{N+2}, \ldots, E_{2N}\right]^T \tag{3.8}$$

to be zero. Its elements are obtained as Hankel transforms of the two interface conditions (2.10) and (2.11), and take the forms

$$\begin{aligned} E_k &= \int_0^\alpha r J_0\left(j_{0,k}\frac{r}{\alpha}\right)\left[\Phi_1(r,\zeta) + (D-1)\zeta\right] \mathrm{d}r, \\ E_{N+k} &= \int_0^\alpha r J_0\left(j_{0,k}\frac{r}{\alpha}\right)\left[w_1(r,\zeta) - u_1(r,\zeta)\zeta'\right] \mathrm{d}r, \qquad k = 1, 2, \ldots, N. \end{aligned} \tag{3.9}$$

These error terms (3.9) make optimum use of the orthogonality relations for Bessel functions; see [29, p. 485, formula 11.4.5], and indeed, if the problem were a linear one, the use of (3.9) would lead at once to formulae for the unknown coefficients in the vector (3.7). Since the problem is nonlinear, however, iteration is required.

The integrals in the error expressions (3.9) must be evaluated numerically, and this has been done using the composite trapezoidal rule evaluated at mesh points

$$r_k = (k-1)\frac{\alpha}{P-1} \qquad \text{for } k = 1, 2, \ldots, P. \tag{3.10}$$

Because this is a full Galerkin method, there is no relationship between the number of coefficients N and the number of grid points P used in the numerical method.

This scheme works well for larger values of the density ratio $D > 2$, and extensive results have been produced in this parameter range. However, these are generally unrealistically large values of D. For the fresh-water salt-water interface, in particular, density ratios in the interval $1 < \mathrm{D} < 1{\cdot}05$ are typically to be expected; see, for example, [17, p. 21]. This fact introduces an additional difficulty, since it is observed that the mathematical problem becomes ill-conditioned in the steady case, as $D \to 1$, for the physical reason that the interface location varies greatly with small perturbations, for $D \approx 1$. Consequently, a regularization scheme is needed, and we choose in this section to minimize the total curvature κ_T of the interface, which may be represented in the form

$$\kappa_T = \iint_{z=\zeta} \left[\nabla^2\zeta\right]^2 \mathrm{d}A = \int_0^{2\pi}\int_0^\alpha \left[\frac{1}{r}\frac{\mathrm{d}}{\mathrm{d}r}\left(r\frac{\mathrm{d}\zeta}{\mathrm{d}r}\right)\right]^2 r\,\mathrm{d}r\,\mathrm{d}\theta.$$

After use of the series (3.6) and results from the theory of Bessel functions (see [29, p. 485, formula 11.4.5]), we obtain

$$\kappa_T = \frac{\pi}{\alpha^2} \sum_{n=1}^{\infty} B_n^2 \big(j_{0,n}\big)^4 J_1^2\big(j_{0,n}\big). \tag{3.11}$$

To minimize this expression, it is simply required to take

$$\frac{\mathrm{d}\kappa_T}{\mathrm{d}B_k} = \frac{2\pi}{\alpha^2} B_k \big(j_{0,k}\big)^4 J_1^2\big(j_{0,k}\big) = 0. \tag{3.12}$$

Thus the regularized method combines Equation (3.12) with the first of the equations in the system (3.9), to give

$$\begin{aligned} E_k &= \int_0^{\alpha} r J_0\left(j_{0,k}\frac{r}{\alpha}\right)\Big[\Phi_1(r,\zeta) + (D-1)\zeta\Big]\,\mathrm{d}r + \epsilon_1 \frac{2\pi}{\alpha^2} B_k \big(j_{0,k}\big)^4 J_1^2\big(j_{0,k}\big), \\ E_{N+k} &= \int_0^{\alpha} r J_0\left(j_{0,k}\frac{r}{\alpha}\right)\Big[w_1(r,\zeta) - u_1(r,\zeta)\zeta'\Big]\,\mathrm{d}r \qquad k = 1, 2, \ldots, N. \end{aligned} \tag{3.13}$$

A damped Newton's method algorithm is used to update the vector of unknowns (3.7) by forcing the error vector (3.8) to zero; its elements are given in Equation (3.13). Convergence usually occurs within five to ten iterations. It is necessary to experiment with the regularization parameter ϵ_1 in (3.13),to find a value large enough to ensure well-conditioning of the method, but still small enough for the original system (3.9) to be represented accurately. Further details may be found in the book by Delves and Mohamed [27, p. 309].

4. Analysis of the solution

Far away from the coastal region or the withdrawal point at the centre of the island, it is possible to estimate the interface location from the simple formula

$$\zeta(r) \approx -\frac{1}{D-1}. \tag{4.1}$$

Equation (4.1) is known as the Ghyben-Herzberg formula, and may be found in the books by Bouwer [22, p. 402] and Raudkivi and Callander [23, p. 175], for example. It assumes that there is no fluid motion in either the fresh or the salt water layer, and thus that the fresh water floats in hydrostatic balance above the salt water. The result follows as a trivial solution from Equations (2.3) and (2.7), since if there is no fluid motion in the fresh water layer, then Φ_1 must be a constant with the value 1. The dynamical condition (2.11) at the interface then gives Equation (4.1). A detailed discussion of the history and validity of the Ghyben-Herzberg relation (4.1) is given by Holzbecher [17, Section 11.2].

It is possible to derive some simple yet useful results concerning the flow along the interface, on the basis of an analysis of the exact conditions (2.10) and (2.11). These results can be summarized in the following theorem:

THEOREM 1. *Along the interface $z = \zeta(r)$, the fluid velocity vector always has a component directed upwards. Fluid moves back towards the centre if the interface slopes downward, and radially out from the centre if the interface slopes upward. The interface is horizontal at a stagnation point.*

Proof. This result follows from the dynamic interface condition (2.11) written in the form

$$\Phi_1\big(r, \zeta(r)\big) = -(D-1)\zeta(r).$$

The derivative of this equation with respect to the radial coordinate r yields

$$\frac{\partial \Phi_1}{\partial r}(r,\zeta) + \frac{\partial \Phi_1}{\partial z}(r,\zeta)\frac{\mathrm{d}\zeta}{\mathrm{d}r} = -(D-1)\frac{\mathrm{d}\zeta}{\mathrm{d}r}. \tag{4.2}$$

The kinematic condition (2.10) is used to eliminate the derivative $\partial\Phi_1/\partial z$ in Equation (4.2), and velocity components are introduced from Darcy's law (2.3). The result is

$$u_1(r,\zeta) = \frac{(D-1)\zeta'}{1+(\zeta')^2} w_1(r,\zeta) = \frac{(D-1)(\zeta')^2}{1+(\zeta')^2}. \tag{4.3}$$

It follows from Equation (4.3) that $w_1 \geq 0$, and so the vertical component of the fluid is always non-negative. Thus the fluid velocity vector always has an upward component. From (4.3), it is also the case that $u_1 > 0$ if $\zeta' > 0$, and that $u_1 < 0$ if $\zeta' < 0$. Thus the fluid flows radially outward (parallel to the interface) if the interface slopes upward ($\zeta' > 0$), or else flows radially inward if the slope is negative ($\zeta' < 0$). At a stagnation point, where both velocity components in Equation (4.3) are zero, it must be the case that $\zeta' = 0$, so that the interface is horizontal there. This concludes the proof. □

The results of this theorem enable reasonably detailed qualitative descriptions of the flow within the fresh-water lens to be made. In the absence of the extraction sink ($\mu = 0$), the interface will be horizontal at the centre $r = 0$, but then will rise monotonically until it meets the sea water at the height $\zeta = 0$ at the island edge $r = \alpha$, from Equation (2.12). In fact, for an island of large width α, the interface will be almost flat over a large portion near the centre of the island, at the height given by the Ghyben-Herzberg formula (4.1).

For non-zero extraction strength, $\mu \neq 0$, the above theorem shows that the interface must form a stagnation point at some non-zero radius r_s within the island. Over the interval $0 < r < r_s$ the slope of the interface will be negative, and so the fluid will be drawn backwards up the interface, toward the extraction sink. Beyond this radius, in the interval $r_s < r < \alpha$, the slope of the interface will be positive, and so the fresh water will move outward along the interface and escape away from the island. (This is possible in this steady-state problem because there is continual recharge at the top of the island, as expressed by Equation (2.7)). Furthermore, there will be a stagnation streamline, starting at some point at the top of the island, $z = 1$, and connecting to the stagnation point $(r_s, \zeta(r_s))$ on the interface. This streamline will divide the flow region into an inner portion that is ultimately drawn into the extraction sink, and an outer region that eventually flows out of the island through the sides.

5. Near-field solution for island of great width

The problem as posed in Sections 2 and 3, for an island of finite radius α, is ill-conditioned for $D \approx 1$. This is also exacerbated by the fact that, over much of the island, the interface $z = \zeta(r)$ is nearly flat, with elevation given by the Ghyben-Herzberg formula (4.1), but rises abruptly to the level $\zeta = 0$ in Equation (2.12) at the edge $r = \alpha$. The numerical difficulties associated with the coastal zone near $r = \alpha$ may be avoided by allowing $\alpha \to \infty$, and focussing instead on the near-field region about $r = 0$. This is equivalent to considering an island of infinite lateral extent.

The total pressure Φ_1 again satisfies Laplace's equation (2.5) and Darcy's law (2.3). The symmetry condition (2.6) holds at the axis $r = 0$, and the top of the island at $z = 1$ remains in contact with the open air, so that the condition (2.7) is still obeyed there. Again, the limiting behaviour (2.9) applies near the sink at the point $(r, z) = (0, \lambda)$. At the interface $z = \zeta(r)$, there is the kinematic requirement expressed by Equation (2.10) and the dynamical condition (2.11). However, the edge condition (2.12) is now replaced by the Ghyben-Herzberg law

$$\zeta(r) \to -\frac{1}{D-1} \qquad \text{as } r \to \infty. \tag{5.1}$$

This new problem is amenable to solution using a boundary-integral method, particularly as the source of ill-conditioning in the problem has been greatly reduced by the use of the condition (5.1). Suppose that a fixed point Q is defined on the unknown interface $z = \zeta$, and a moveable point P is on one of the surfaces of the fresh water in region 1, including the interface itself. By Green's second identity, it then follows that

$$\iint_{\partial V_1} \left(\Phi_1(P) \frac{\partial G}{\partial n_P} - G \frac{\partial \Phi_1(P)}{\partial n_P} \right) \mathrm{d}S_P = 0, \tag{5.2}$$

since both the potential Φ_1 and the Green function $G(P, Q)$ satisfy Laplace's equation in the volume V_1 occupied by the fresh water in upper layer 1.

The boundary ∂V_1 of volume V_1 consists of the upper surface $z = 1$, a cylindrical surface of infinite radius in the region $-1/(D-1) < z < 1$, and the interfacial surface $z = \zeta$ punctured by a small circular disk of radius ϵ about the point Q. There is also a hemispherical surface S_Q, of radius ϵ, that is centred at point Q and excludes it from the volume V_1. In addition, the sink point $(r, \theta) = (0, \lambda)$ is likewise excluded from volume V_1 by the small spherical surface S_λ centred at this point. A sketch of volume V_1 and its boundary surfaces is given in Figure 2.

The Green function G in Equation (5.2) is now chosen to be

$$\begin{aligned} G(P, Q) \;=\; & \frac{1}{\sqrt{r_P^2 + r_Q^2 - 2 r_P r_Q \cos(\theta_P - \theta_Q) + (z_P - z_Q)^2}} \\ & - \frac{1}{\sqrt{r_P^2 + r_Q^2 - 2 r_P r_Q \cos(\theta_P - \theta_Q) + (z_P + z_Q - 2)^2}}. \end{aligned} \tag{5.3}$$

This function has the property that it vanishes on the top surface $z = 1$, and becomes singular as $P \to Q$.

The contribution to the integral in Equation (5.2) from each of the component surfaces that make up the boundary ∂V_1 is now assessed, and it may be shown that the total pressure head Φ_1 along the interface satisfies the integral equation

$$\begin{aligned} 2\pi \Phi_1(Q) + \iint_{z=\zeta} \Phi_1(P) \frac{\partial G}{\partial n_P} \mathrm{d}S_P \;=\; & -\mu \left[\frac{1}{\sqrt{r_Q^2 + (\lambda - \zeta_Q)^2}} - \frac{1}{\sqrt{r_Q^2 + (\lambda + \zeta_Q - 2)^2}} \right] \\ & - \iint_{z=1} \frac{\partial G}{\partial n_P} \mathrm{d}S_P, \end{aligned} \tag{5.4}$$

in which $G(P, Q)$ is the Green function in Equation (5.3).

The integral on the left-hand side of Equation (5.4) is strongly singular as $P \to Q$, since it involves the normal derivative of the Green function in Equation (5.3), at the interface $z = \zeta$. It is advantageous to remove the singularity from the integrand of this term by subtraction, using the identity

$$\iint_{z=\zeta} \Phi_1(P) \frac{\partial G}{\partial n_P} \, \mathrm{d}S_P = \iint_{z=\zeta} \big[\Phi_1(P) - \Phi_1(Q)\big] \frac{\partial G}{\partial n_P} \, \mathrm{d}S_P + \Phi_1(Q) \iint_{z=\zeta} \frac{\partial G}{\partial n_P} \, \mathrm{d}S_P. \tag{5.5}$$

It is possible to express the last integral on the right-hand side (evaluated over the unknown interface location) in terms of an integral taken over the top surface $z = 1$, using Gauss's theorem

$$\iint_{\partial V_1} \frac{\partial G}{\partial n_P} \, \mathrm{d}S_P = 0,$$

and assessing the contributions made by each of the surfaces that make up the boundary ∂V_1 shown in Figure 2. When the result is combined with the expression (5.5), the singular integral is now seen to take the form

$$\begin{aligned} \iint_{z=\zeta} \Phi_1(P) \frac{\partial G}{\partial n_P} \, \mathrm{d}S_P \;=\; & \iint_{z=\zeta} \big[\Phi_1(P) - \Phi_1(Q)\big] \frac{\partial G}{\partial n_P} \, \mathrm{d}S_P \\ & + \Phi_1(Q) \left[-2\pi - \iint_{z=1} \frac{\partial G}{\partial z_P} \, \mathrm{d}S_P \right]. \end{aligned} \tag{5.6}$$

This result (5.6) is now substituted in the integral equation (5.4), to give the de-singularized expression

$$\begin{aligned} & \big(1 - \Phi_1(Q)\big) \iint_{z=1} \frac{\partial G}{\partial z_P} \, \mathrm{d}S_P + \iint_{z=\zeta} \big[\Phi_1(P) - \Phi_1(Q)\big] \frac{\partial G}{\partial n_P} \, \mathrm{d}S_P \\ & \qquad = -\mu \left[\frac{1}{\sqrt{r_Q^2 + (\lambda - \zeta_Q)^2}} - \frac{1}{\sqrt{r_Q^2 + (\lambda + \zeta_Q - 2)^2}} \right]. \end{aligned} \tag{5.7}$$

The integral in the first term on the left-hand side of Equation (5.7) can in fact be evaluated in closed form, to give

$$\iint_{z=1} \frac{\partial G}{\partial z_P} \, \mathrm{d}S_P = -4\pi. \tag{5.8}$$

This result is discussed further in the Appendix. The integral equation for determining the pressure head Φ_1 along the unknown interface therefore takes the form

$$\begin{aligned} & -4\pi \big(1 - \Phi_1(Q)\big) + \iint_{z=\zeta} \big[\Phi_1(P) - \Phi_1(Q)\big] \frac{\partial G}{\partial n_P} \, \mathrm{d}S_P \\ & \quad + \mu \left[\frac{1}{\sqrt{r_Q^2 + (\lambda - \zeta_Q)^2}} - \frac{1}{\sqrt{r_Q^2 + (\lambda + \zeta_Q - 2)^2}} \right] = 0. \end{aligned} \tag{5.9}$$

The interface profile $z = \zeta(r)$ and the potential function $\Phi_1(r)$ are both axisymmetric functions, and this allows one of the integrations (in the azimuthal coordinate θ) to be performed explicitly, in the double-integral term in Equation (5.9). The required transformations

are given in the paper by Forbes and Hocking [5] and will not be repeated here. After some algebra, the integral equation (5.9) may be expressed in the final form

$$\int_0^\infty \big[\Phi_1(P) - \Phi_1(Q)\big]\mathbb{K}(a_2, b, c_2, d)\,\mathrm{d}r_P - \int_0^\infty \big[\Phi_1(P) - \Phi_1(Q)\big]\mathbb{K}(a_1, b, c_1, d)\,\mathrm{d}r_P$$

$$+ \mu\left[\frac{1}{\sqrt{r_Q^2 + (\lambda - \zeta_Q)^2}} - \frac{1}{\sqrt{r_Q^2 + (\lambda + \zeta_Q - 2)^2}}\right] - 4\pi\big(1 - \Phi_1(Q)\big) = 0. \tag{5.10}$$

The kernel in this integral equation is defined to be

$$\mathbb{K}(a, b, c, d) = r_p \int_0^{2\pi} \frac{a - b\cos\theta}{[c - d\cos\theta]^{3/2}}\,\mathrm{d}\theta \tag{5.11}$$

and the six auxiliary functions in Equation (5.10) are

$$a_1 = r_P\zeta_P' - (\zeta_P - \zeta_Q), \quad a_2 = r_P\zeta_P' - (\zeta_P + \zeta_Q - 2), \quad b = r_Q\zeta_P',$$

$$c_1 = r_P^2 + r_Q^2 + (\zeta_P - \zeta_Q)^2, \quad c_2 = r_P^2 + r_Q^2 + (\zeta_P + \zeta_Q - 2)^2, \quad d = 2r_Pr_Q.$$

Forbes and Hocking [5] have shown that the kernel in Equation (5.11) can be expressed in terms of complete elliptic integrals K and E, of the first and second kind respectively, according to the formula

$$\mathbb{K}(a, b, c, d) = \frac{2}{\sqrt{c + d}}\left[\zeta_P' K\big(\frac{2d}{c + d}\big) + \big(\frac{2ar_P - \zeta_P' c}{c - d}\big)E\big(\frac{2d}{c + d}\big)\right]. \tag{5.12}$$

Expressions somewhat similar to Equation (5.12) are also given in [30, Chapter 6]. The complete elliptic integrals K and E are straightforward to evaluate numerically, and expressions for doing so are given by Liggett and Liu, based on the formulae in [29, p. 591].

The numerical solution of the integral equation (5.10), subject to the interfacial surface condition (2.11) and the far-field condition (5.1), is now accomplished by a Newton method approach similar to that outlined in Section 3. A grid of N points is placed along the interface, at locations

$$r_k = (k - 1)\Delta r, \qquad k = 1, 2, \ldots, N$$

and a vector of unknowns $\mathbf{u}$ of length $N - 1$ is created from interface elevations at all mesh points except the last. This vector is therefore

$$\mathbf{u} = \big[\zeta_1, \zeta_2, \ldots, \zeta_{N-1}\big]^T. \tag{5.13}$$

At the last point downstream, the interface elevation is taken to be $\zeta_N = -1/(D - 1)$, so as to satisfy condition (5.1). The derivatives ζ_k', $k = 1, 2, \ldots, N$ are computed from the vector (5.13) of unknowns using Lagrangian five-point differentiation formulae, and the total pressure Φ_k is computed at each mesh point using Equation (2.11).

The integral equation (5.10) is evaluated at the $N - 1$ half-grid points

$$r_{k+1/2} = \frac{1}{2}\big(r_k + r_{k+1}\big), \qquad k = 1, 2, \ldots, N - 1. \tag{5.14}$$

At these points, the interface height is estimated using interpolation, according to the simple formula

$$\zeta_{k+1/2} = \frac{1}{2}\big(\zeta_k + \zeta_{k+1}\big)$$

and the potential $\Phi_{k+1/2}$ at these half-mesh points is then calculated directly from Equation (2.11). As in Section 3, an error vector $\mathbf{E}$ is created, having length $N-1$, and its components are the integral equation (5.10) evaluated at the points in Equation (5.14). When trapezoidal-rule quadrature is used to approximate the integrals, the components of the error vector are therefore determined to be

$$\begin{aligned} E_k \;=\; & \Delta r \sum_{j=1}^{N} w_j\big(\Phi_j - \Phi_{k+1/2}\big)\mathbb{K}(a_2, b, c_2, d) - \Delta r \sum_{j=1}^{N} w_j\big(\Phi_j - \Phi_{k+1/2}\big)\mathbb{K}(a_1, b, c_1, d) \\ & + \mu\left[\frac{1}{\sqrt{r_{k+1/2}^2 + (\lambda - \zeta_{k+1/2})^2}} - \frac{1}{\sqrt{r_{k+1/2}^2 + (\lambda + \zeta_{k+1/2} - 2)^2}}\right] \\ & - 4\pi\big(1 - \Phi_{k+1/2}\big), \qquad k = 1, 2, \ldots, N-1. \end{aligned} \tag{5.15}$$

In this expression, the quantities w_j are the weights appropriate for trapezoidal-rule integration. They have the values $w_j = 1/2$ if $j = 1, N$ and $w_j = 1$ if $2 \leqslant j \leqslant N-1$.

Newton's method is used to update the vector of unknowns in Equation (5.13) iteratively, by driving to zero the error vector, with components given in Equation (5.15). The method generally converges quickly, with four or five iterations needed to produce a final solution.

The numerical method for solving the integral equation (5.10) outlined above is ill-conditioned for $D \approx 1$, for the reasons outlined in Section 3. Accordingly, it is useful to add a regularization term to the error components in Equation (5.15). One measure of the total deflection of the interface is the term

$$\iint_{z=\zeta} \big[\sqrt{1 + |\nabla\zeta|^2} - 1\big]\,\mathrm{d}A = 2\pi \int_0^\infty \big[\sqrt{1 + \zeta_r^2} - 1\big]\, r\,\mathrm{d}r$$

and the calculus of variations indicates that this deflection is minimized by the Euler equation

$$\frac{\mathrm{d}}{\mathrm{d}r}\left(\frac{r\zeta_r}{\sqrt{1 + \zeta_r^2}}\right) = 0.$$

Thus the term

$$\epsilon_1\left[\frac{\zeta'_{k+1/2}}{\sqrt{1 + (\zeta'_{k+1/2})^2}} + \frac{r_{k+1/2}\zeta''_{k+1/2}}{[1 + (\zeta'_{k+1/2})^2]^{3/2}}\right] \tag{5.16}$$

is added to the components of the error vector, given in Equation (5.15). This modification is capable of reducing the oscillations in the interface profile that are typical of the errors produced by ill-conditioning. The regularization parameter ϵ_1 in Equation (5.16) must again be determined by numerical experimentation.

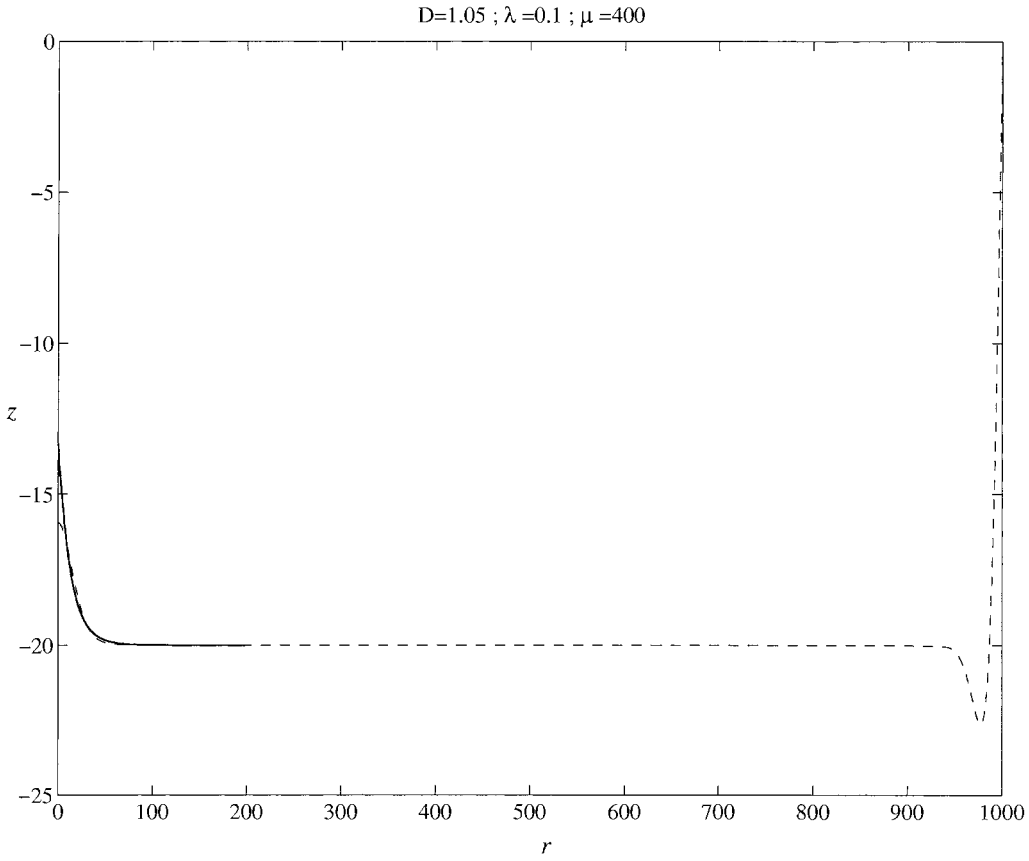

Figure 3. A comparison of the numerical solution for the interfacial surface, obtained with the full spectral solution (dashed line, for island radius $\alpha = 1000$), and the integral equation technique (solid line) valid in the near field. The density ratio is $D = 1{\cdot}05$, and the sink height and strength are respectively $\lambda = 0{\cdot}1$ and $\mu = 400$.

6. Presentation of results

The spectral solution technique of Section 3 and the integral equation approach of Section 5 (valid closer to the island's centre) have both been run for a wide variety of parameter values. Convergence has usually been found to be good, in the sense that the numerical results are insensitive to numerical parameters such as grid spacing. Nevertheless, this steady problem becomes ill-conditioned as $D \to 1$, which is the case of most interest; see [17, p. 21]. This is associated with grid-scale oscillations in the numerical results. These may be controlled in the numerical solution by the regularization methods introduced in Sections 3 and 5, and experimentation suggests that appropriate values of the regularization parameter ϵ_1 are of the order of 1. When the island is of finite radius α, the abrupt rise in the interface elevation in the coastal zone, from the Ghyben-Herzberg depth (4.1) to zero, as indicated in Equation (2.12), can also cause spurious oscillations in the interface location. These are related to the Gibbs phenomenon in the Fourier-Bessel series representations (3.5) and (3.6). These oscillations are likewise mostly suppressed by the regularization strategy discussed above.

In Figure 3, the interface is presented for an island of radius $\alpha = 1000$, with an extraction point at $\lambda = 0{\cdot}1$ (which is slightly higher than the external sea-water level). The sink extraction rate parameter is $\mu = 400$ and the density ratio of fresh to salt water is $D = 1{\cdot}05$.

The interface is drawn with a dashed line, and over most of the island, is flat at the Ghyben-Herzberg depth (4.1). Near the extraction point at the centre of the island, the interface rises rather sharply, as is to be expected. At the edge of the island, near $r = \alpha$, a dip may be seen in the interface profile. This is, in fact, a spurious feature related to the oscillations caused by the Gibbs phenomenon. When the regularization parameter ϵ_1 in Equation (3.13) is reduced, a sequence of oscillations appears in this coastal zone, and the dip evident in Figure 3 is merely the first trough in this pattern. However, the value $\epsilon_1 = 1$ of the regularization parameter used here is just sufficient to suppress all oscillations except the first. Beyond the numerical dip, the interface rises to the sea-water height at the edge of the island, in accordance with the condition (2.12). This solution was computed with $N = 201$ coefficients and $P = 801$ numerical grid points along the interface.

Also shown on Figure 3 is the near-field solution for the same parameter values, computed with the integral-equation technique discussed in Section 5. This is drawn with a solid line. For the most part, the agreement with the spectral solution is good, although the near-field solution rises higher at the extraction location $r = 0$. The regularization process applied to the spectral method tends to damp the interface close to the extraction zone, and this is evident in Figure 3.

The spectral solution method in Section 3 permits the fluid velocity vector components u_1 and w_1 within the island to be calculated directly, by straightforward differentiation of the potential Φ_1 in Equation (3.5). It is found that over much of the island the velocity vector is nearly zero, except near the sink at $(0, \lambda)$ and the waterline at $(\alpha, 0)$ when fluid speeds can be large. Consequently it is difficult to visualize the velocity vector field in a meaningful way.

It is therefore more instructive to compute the Stokes stream function $\Psi_1(r, z)$, from the two velocity components u_1 and w_1 in the radial and vertical directions, and plot streamlines. These have the property that they are everywhere parallel to the fluid velocity vector, and so provide an excellent tool for the visualization of the flow field. The Stokes stream function Ψ_1 is obtained from the relations

$$u_1 = \frac{\partial \Psi_1}{\partial z} \qquad \text{and} \qquad w_1 = -\frac{1}{r}\frac{\partial}{\partial r}\big(r\Psi_1\big),$$

which after some algebra give the expression

$$\begin{aligned}\Psi_1(r,z) \;=\; & \frac{1}{2}r + \frac{\mu}{4\pi r}\left[\frac{(z-2+\lambda)}{\sqrt{r^2+(z-2+\lambda)^2}} - \frac{(z-\lambda)}{\sqrt{r^2+(z-\lambda)^2}}\right] \\ & - \frac{\mu}{\pi^2}\int_0^\infty \frac{I_1(\omega r)}{I_0(\omega\alpha)} K_0(\omega\alpha)\cos\big(\omega(z-1)\big)\sin\big(\omega(1-\lambda)\big)\,\mathrm{d}\omega \\ & - \sum_{n=1}^{\infty} C_n J_1\left(j_{0,n}\frac{r}{\alpha}\right)\cosh\left(j_{0,n}\frac{1-z}{\alpha}\right). \end{aligned} \tag{6.1a}$$

In this formula, the function J_1 is a Bessel function of the first kind of order 1, and the symbols I_ν and K_ν denote modified Bessel functions, as in Section 3. It follows from a careful analysis of Equation (6.1a) that

$$\lim_{r\to 0} \Psi_1(r, z) = 0, \tag{6.1b}$$

except at the sink point $(r, z) = (0, \lambda)$ where it is undefined.

The stream function Ψ_1 is evaluated from Equations (6.1) at a grid of numerical points within the island. Contours are then drawn for this function, and this at once yields the

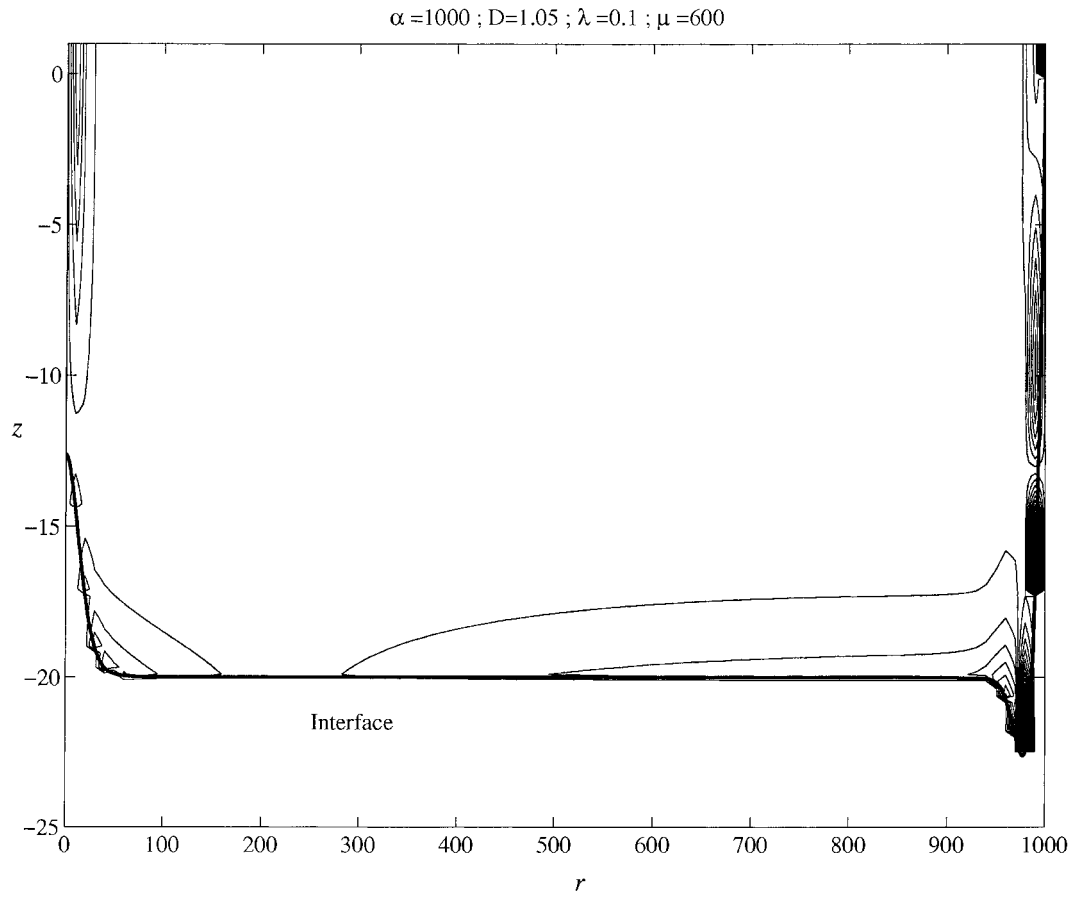

Figure 4. Streamlines computed using the spectral solution method, for an island of radius $\alpha = 1000$ with density ratio $D = 1{\cdot}05$, sink height $\lambda = 0{\cdot}1$ and strength $\mu = 600$. The thicker line towards the bottom of the picture is the interface between the fresh and salty water.

streamlines for fluid flow within the island. An example is shown in Figure 4, for density ratio $D = 1{\cdot}05$, extraction point $\lambda = 0{\cdot}1$ and sink strength parameter $\mu = 600$, computed for an island of radius $\alpha = 1000$. Here, the streamlines are drawn using equally-spaced increments in Ψ_1. The thicker line near the bottom of Figure 4 is the interface $z = \zeta(r)$.

Over much of the island's interior, the stream function in Equation (6.1a) is almost zero, and the fluid seepage velocity components are very small. For this reason, streamlines are not evident over much of the interior region in Figure 4. Fluid seepage speed is greatest near the centre of the island, as might be expected on purely geometrical grounds, and this is reflected by the clustering of streamlines near $r = 0$. It is also apparent from Figure 4 that the streamlines near the centre $r = 0$ first descend from the top surface $z = 1$ of the island and then curve back upwards toward the extraction point at $(r, z) = (0, \lambda)$. This is as would be expected on physical grounds, and is also consistent with the theorem in Section 4, in which Equations (4.3) show how the fluid velocity at the interface near $r = 0$ must be directed upwards and back toward the centre.

At the edge $r = \alpha$ of the island, streamlines likewise move downwards from the top surface $z = 1$, and ultimately move outwards through the side wall. This reflects the fact that the fresh

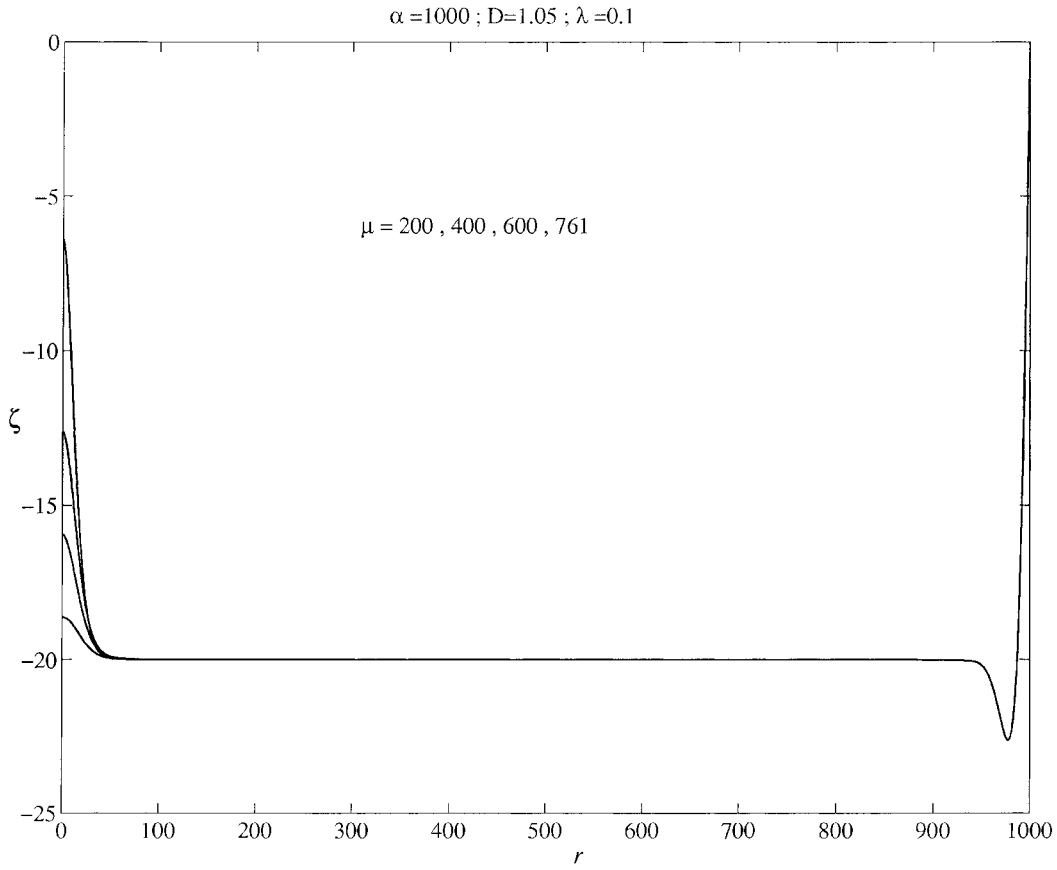

Figure 5. Four different interface profiles, for the case $\alpha = 1000$, $D = 1{\cdot}05$ and $\lambda = 0{\cdot}1$, for the four extraction sink strengths $\mu = 200$, 400, 600 and 761.

water enters the top of the island, soaks down under the effect of gravity and finally seeps out through the porous rock at the island's edge. Some minor evidence of oscillations in the streamlines is evident near the extraction zone and the coastal zone at the edge of the island, but this is a small error associated with Gibbs's phenomenon.

From the discussion in Section 4, there must be a stagnation zone on the interface at some non-zero radius r_s and from Figure 4, it is evident that this occurs very approximately at $r_s \approx 200$. There must be some streamline, starting at the top of the island and connecting to the stagnation point $(r_s, \zeta(r_s))$, that divides the flow in Figure 4 into two regions. The inner region is ultimately drawn into the extraction sink at $(r, z) = (0, \lambda)$ and the outer flow ultimately exits through the side wall $r = \alpha$ of the island.

To conclude this presentation of results, four interface profiles are displayed in Figure 5, for this steady-state solution. The island radius is $\alpha = 1000$ and the density ratio is again $D = 1{\cdot}05$. The solutions shown are for the four different values of the sink strength $\mu = 200$, 400, 600 and 761, and the biggest of these represents the largest extraction rate μ for which the solution technique of Section 3 could yield a steady solution. Each interface profile is roughly horizontal at the Ghyben-Herzberg depth (4.1) over much of the island, but each rises to a maximum at $r = 0$. Near the coastal zone $r = \alpha$, the interfaces rise abruptly to the sea

level $z = 0$, although there is a numerically-generated dip in the interface near the island's edge, that is related to the Gibbs's phenomenon, as discussed above.

The numerical scheme in Section 3 does not yield a solution for $\mu > 761$, and a similar result is obtained from the near-field solutions described in Section 5. No solutions have been obtained for which the interface is drawn right up into the extraction point at $z = \lambda$, and so it remains uncertain as to whether such steady configurations are possible. In the analogous 'water coning' problem in the extraction of oil from a horizontal layer beneath which a water table is present, the steady two-dimensional solutions of Zhang *et al.* [14] and the corresponding three-dimensional solutions obtained by Lucas and Kucera [13] also produced a limiting steady interface profile with an upward vertical cusp below the extraction sink, and it is possible that the same situation may occur here also.

7. Discussion and conclusion

The shape of the interface between an upper fresh water layer and a stationary lower layer of salt water in a tropical island has been studied in this paper. Steady-state solutions (independent of time) have been sought, and the effect of withdrawing fluid from the upper layer of fresh water has been investigated. It is assumed that the fresh water layer is recharged through rainfall at the top of the island, and that the rainfall is so plentiful that the top of the fresh water aquifer coincides with the top of the island. The excess rainfall that cannot percolate down into the island simply runs off into the ocean, and does so on a time scale much shorter than typical time scales associated with groundwater movement.

Over much of the island, the interface is found to be flat, at a height given by the classical Ghyben-Herzberg relation (which simply expresses a hydrostatic balance between upper and lower stationary layers of fluid). This is largely a result of the fact that the island width is large by comparison with the Ghyben-Herzberg depth in Equation (4.1), and indeed this ratio is infinite for the results obtained with the methods of Section 5. The interface rises rapidly to the sea-surface level $z = 0$ at the edge of the island $r = \alpha$, which is in accordance with approximate theories presented by Bear [10, pp. 559–563] for example, which predict that the interface has the form of an inverse parabola. For islands of large width, there is an approximate de-coupling of the withdrawal region near $r = 0$ from the coastal effects near $r = \alpha$, as is evident from the streamline pattern in Figure 4.

Near the extraction region in the centre of the island, the interface is drawn upwards towards the extraction point. For sufficiently large pumping rate, the steady solutions obtained numerically eventually fail, and so it remains unclear what physically occurs at larger pumping rates. One possibility is that there is a limiting steady solution with a vertical cusp formed at some maximum height that is nevertheless below the extraction point. Such solutions were found in a related problem by Lucas and Kucera [13]. In that case, the flow for larger pumping rates would become unsteady, and the interface would be drawn intermittently into the extraction well, so giving bursts during which break-through would occur and both fluids would be withdrawn simultaneously. Alternatively, it is possible that steady solutions are possible, for which both fluids are withdrawn simultaneously and the interface passes into the extraction point. Solutions of this form have been found in related problems by Lister [7], Hocking [4] and Forbes [15]. The present numerical schemes are not able to resolve this question directly, particularly as the regularization process necessary for their stability tends to smooth the interface at the extraction zone. This question therefore awaits further research.

A difficulty with the solution methods presented here is that they are found to be ill-conditioned as the density ratio D becomes close to 1, which is the situation occurring in practice. Numerically, this becomes evident from a study of the Jacobian matrix in Newton's method, which is found to have a high condition number, and also from the presence of grid-scale oscillations in the results, which become more pronounced as more grid points are used. This problem is well documented in groundwater literature, and the paper by Wikramaratna and Wood [28], for example, discusses this in some detail. In the present paper, the problem has been overcome to a large extent by the careful use of a Tikhonov regularization strategy, although this can introduce undesirable smoothing precisely in regions of most interest, such as the extraction zone.

In principle, this difficulty with ill-conditioning is a consequence of the fact that we have sought steady-state solutions that are independent of time. Nevertheless, we have argued in this paper that the mathematical ill-conditioning of the results reflects physical reality, and is a consequence of the very small difference in density between the upper fresh water and the lower salty layer. It follows, therefore, that comparable difficulties will be encountered with solution methods that advance the flow forward in time. This is indeed the case, and the numerical oscillations encountered here in the steady solution, related to the Gibbs phenomenon, have a counterpart in unsteady solution techniques, where numerical overshoot of the steady-state configuration is observed [17]. It has likewise been observed that, in practice, it can take 10 to 20 years for an aquifer to adjust to the steady-state height predicted by the Ghyben-Herzberg relation (see [17, Section 11.2]), and this is the physical manifestation of the ill-conditioning reported here.

In this paper, the extra complexity associated with an upper free surface for the fresh-water layer has been avoided by assuming that rainfall is so plentiful that the entire island is saturated, and the groundwater surface occurs at the top of the island. In many practical situations this will not be the case, however, and a free surface will be present above the fresh water, in addition to the interface beneath it. The same numerical difficulties have been encountered for that problem also, and will be discussed in a future article.

Appendix – Evaluation of integral across top of island

When the integral on the left-hand side of Equation (5.8) is written out in full, making use of the definition of the Green function in Equation (5.3), it may be seen that

$$\iint_{z=1} \frac{\partial G}{\partial z_P}\,\mathrm{d}S_P = -2(1-z_Q)\int_0^{2\pi}\mathrm{d}\theta_P \int_0^{\infty} \frac{r_P\,\mathrm{d}r_P}{[r_P^2 - 2r_P C_T + D_T]^{3/2}}, \tag{A1}$$

in which it is convenient temporarily to define the auxiliary functions

$$C_T = r_Q\cos(\theta_P - \theta_Q), \qquad D_T = r_Q^2 + (1-z_Q)^2. \tag{A2}$$

The inner integral in Equation (A1) can be evaluated in closed form, and after a little algebra the result is found to be

$$\iint_{z=1} \frac{\partial G}{\partial z_P}\,\mathrm{d}S_P = -2(1-z_Q)\int_0^{2\pi}\mathrm{d}\theta_P \frac{C_T + \sqrt{D_T}}{D_T - C_T^2}. \tag{A3}$$

The intermediate functions C_T and D_T are now replaced in Equation (A3) by their definitions from (A2). It is possible also to remove the quantity θ_Q from the integral, since the integrand

is a periodic function and it is integrated over a complete period. Equation (A3) can now be expressed in the form

$$\iint_{z=1} \frac{\partial G}{\partial z_P}\,\mathrm{d}S_P = -2B\int_0^{2\pi} \frac{A\cos\theta + C}{A^2\sin^2\theta + B^2}\,\mathrm{d}\theta, \tag{A4}$$

in which we have defined

$$A = r_Q, \qquad B = 1 - z_Q, \qquad C = \sqrt{A^2 + B^2}. \tag{A5}$$

The integral in Equation (A4) can be evaluated using the residue theorem. The calculation is straightforward, and after some algebra, Equation (A4) yields

$$\iint_{z=1} \frac{\partial G}{\partial z_P}\,\mathrm{d}S_P = -2B\frac{2\pi C}{B\sqrt{A^2 + B^2}}.$$

When the quantities A, B and C are eliminated using Equation (A5), the result in Equation (5.8) in the text follows.

References

1. E.O. Tuck and J.-M. Vanden-Broeck, A cusp-like free-surface flow due to a submerged source or sink. *J. Austral. Math. Soc. Ser. B* 25 (1984) 443–450.
2. G.C. Hocking and L.K. Forbes, A note on the flow induced by a line sink beneath a free surface. *J. Austral. Math. Soc. Ser. B* 32 (1991) 251–260.
3. L.K. Forbes and G.C. Hocking, Flow induced by a line sink in a quiescent fluid with surface-tension effects. *J. Austral. Math. Soc. Ser. B* 34 (1993) 377–391.
4. G.C. Hocking, Supercritical withdrawal from a two-layer fluid through a line sink. *J. Fluid Mech.* 297 (1995) 37–47.
5. L.K. Forbes and G.C. Hocking, Flow caused by a point sink in a fluid having a free surface. *J. Austral. Math. Soc. Ser. B* 32 (1990) 231–249.
6. L.K. Forbes and G.C. Hocking, On the computation of steady axi-symmetric withdrawal from a two-layer fluid. *Comp. Fluids* 32 (2003) 385–401.
7. J.R. Lister, Selective withdrawal from a viscous two-layer system. *J. Fluid Mech.* 198 (1989) 231–254.
8. T.J. Singler and J.F. Geer, A hybrid perturbation-Galerkin solution to a problem in selective withdrawal. *Phys. Fluids Ser. A* 5 (1993) 1156–1166.
9. M. Muskat, *The Flow of Homogeneous Fluids Through Porous Media.* New York: McGraw-Hill (1937) 763 pp.
10. J. Bear, *Dynamics of Fluids in Porous Media.* New York: Elsevier (1972) 764 pp.
11. G. Dagan, *Flow and Transport in Porous Formations.* Berlin: Springer-Verlag (1989) 465 pp.
12. S.K. Lucas, J.R. Blake and A. Kucera, A boundary-integral method applied to water coning in oil reservoirs. *J. Austral. Math. Soc. Ser. B* 32 (1991) 261–283.
13. S.K. Lucas and A. Kucera, A boundary integral method applied to the 3D water coning problem. *Phys. Fluids* 8 (1996) 3008–3022.
14. H. Zhang, G.C. Hocking and D.A. Barry, An analytical solution for critical withdrawal of layered fluid through a line sink in a porous medium. *J. Austral. Math. Soc. Ser. B* 39 (1997) 271–279.
15. L.K. Forbes, The design of a full-scale industrial mineral leaching process. *Appl. Math. Modell.* 25 (2001) 233–256.
16. T.S. Ma, M. Sophocleous, Y.-S. Yu and R.W. Buddemeier, Modeling saltwater upconing in a freshwater aquifer in south-central Kansas. *J. Hydrology* 201 (1997) 120–137.
17. E. Holzbecher, *Modeling Density-Driven Flow in Porous Media.* Berlin: Springer-Verlag (1998) 286 pp.
18. P.S. Huyakorn, Y.S. Wu and N.S. Park, Multiphase approach to the numerical solution of a sharp interface saltwater intrusion problem. *Water Resources Res.* 32 (1996) 93–102.

19. J.W. Bower, L.H. Motz and D.W. Durden, Analytical solution for determining the critical condition of saltwater upconing in a leaky artesian aquifer. *J. Hydrology* 221 (1999) 43–54.
20. C.D. Langevin, M.T. Stewart and C.M. Beaudoin, Effects of sea water canals on fresh water resources: an example from Big Pine Key, Florida. *Ground Water* 36 (1998) 503–513.
21. C. Ruppel, G. Schultz and S. Kruse, Anomalous fresh water lens morphology on a strip barrier island. *Ground Water* 38 (2000) 872–881.
22. H. Bouwer, *Groundwater Hydrology.* New York: McGraw-Hill (1978) 480 pp.
23. A.J. Raudkivi and R.A. Callander, *Analysis of Groundwater Flow.* London: Edward Arnold (1976) 214 pp.
24. H.I. Essaid, A comparison of the coupled fresh water-salt water flow and the Ghyben-Herzberg sharp interface approaches to modeling of transient behavior in coastal aquifer systems. *J. Hydrology* 86 (1986) 169–193.
25. D.A. Nutbrown, Optimal pumping regimes in an unconfined coastal aquifer. *J. Hydrology* 31 (1976) 271–280.
26. F. Padilla and J. Cruz-Sanjulián, Modeling sea-water intrusion with open boundary conditions. *Ground Water* 35 (1997) 704–712.
27. L.M. Delves and J.L. Mohamed, *Computational Methods for Integral Equations.* Cambridge: Cambridge University Press (1985) 339 pp.
28. R.S. Wikramaratna and W.L. Wood, Control of spurious oscillations in the salt water intrusion problem. *Int. J. Numer. Meth. Eng.* 19 (1983) 1243–1251.
29. M. Abramowitz and I.A. Stegun (eds.), *Handbook of Mathematical Functions.* New York: Dover (1972) 1046 pp.
30. J.A. Liggett and P. L.-F. Liu, *The Boundary Integral Equation Method for Porous Media Flow.* London: Allen and Unwin (1983) 255 pp.